Cellular/Molecular

Mechanisms That Underlie Expression of Estradiol-Induced Excitatory Synaptic Potentiation in the Hippocampus Differ between Males and Females

Anant Jain and Catherine S. Woolley
Department of Neurobiology, Northwestern University, Evanston, Illinois 60208

17β-estradiol (E2) is synthesized in the hippocampus of both sexes and acutely potentiates excitatory synapses in each sex. Previously, we found that the mechanisms for initiation of E2-induced synaptic potentiation differ between males and females, including in the molecular signaling involved. Here, we used electrical stimulation and two-photon glutamate uncaging in hippocampal slices from adult male and female rats to investigate whether the downstream consequences of distinct molecular signaling remain different between the sexes or converge to the same mechanism(s) of expression of potentiation. This showed that synaptic activity is necessary for expression of E2-induced potentiation in females but not males, which paralleled a sex-specific requirement in females for calcium-permeable AMPARs (cpAMPARs) to stabilize potentiation. Nonstationary fluctuation analysis of two-photon evoked unitary synaptic currents showed that the postsynaptic component of E2-induced potentiation occurs either through an increase in AMPAR conductance or in nonconductive properties of AMPARs (number of channels × open probability) and never both at the same synapse. In females, most synapses (76%) were potentiated via increased AMPAR conductance, whereas in males, more synapses (60%) were potentiated via an increase in nonconductive AMPAR properties. Inhibition of cpAMPARs eliminated E2-induced synaptic potentiation in females, whereas some synapses in males were unaffected by cpAMPAR inhibition; these synapses in males potentiated exclusively via increased AMPAR nonconductive properties. This sex bias in expression mechanisms of E2-induced synaptic potentiation underscores the concept of latent sex differences in mechanisms of synaptic plasticity in which the same outcome in each sex is achieved through distinct underlying mechanisms.

Key words: **AMPA receptor; neurosteroid; plasticity; sex difference; synapse**

Significance Statement

Estrogens are synthesized in the brains of both sexes and potentiate excitatory synapses to the same degree in each sex. Despite this apparent similarity, the molecular signaling that initiates estrogen-induced synaptic potentiation differs between the sexes. Here we show that these differences extend to the mechanisms of expression of synaptic potentiation and result in distinct patterns of postsynaptic neurotransmitter receptor modulation in each sex. Such latent sex differences, in which the same outcome is achieved through distinct underlying mechanisms in males versus females, indicate that molecular mechanisms targeted for drug development may differ between the sexes even in the absence of an overt sex difference in behavior or disease.

Introduction

In addition to its roles as a hormone, 17β-estradiol (E2) can be rapidly synthesized as a neurosteroid in the hippocampus (Hojo et al., 2004, 2009; Sato and Woolley, 2016; Tuscher et al., 2016) where it acutely modulates both excitatory (Teyler et al., 1980; Wong and Moss, 1992; Kramar et al., 2009; Smejkalova and Woolley, 2010; Jain et al., 2019) and inhibitory (Huang and Woolley, 2012; Tabatadze et al., 2015) synapses. For example, E2 acutely potentiates excitatory synaptic transmission at a subset of CA3-CA1 synapses. This occurs in both sexes (Jain et al., 2019) and works through synapse-specific presynaptic and postsynaptic changes that occur largely independently (Oberlander and Woolley, 2016). Although the functions of neurosteroid E2 are not yet fully understood, forebrain-selective knockout of the estrogen synthesizing enzyme, aromatase (Lu et al., 2019) or hippocampal infusion of

Received Aug. 27, 2019; revised Jan. 8, 2023; accepted Jan. 9, 2023.
Author contributions: A.J. and C.S.W. designed research; A.J. performed research; A.J. analyzed data; A.J. wrote the first draft of the paper; C.S.W. wrote the paper.
This work was supported by National Institutes of Health grant R01 MH113189 to C.S.W.
The authors declare no competing financial interests.
Correspondence should be addressed to Catherine S. Woolley at cwoolley@northwestern.edu.
https://doi.org/10.1523/JNEUROSCI.2080-19.2023

aromatase inhibitors (Sato and Woolley, 2016; Tuscher et al., 2016; Marbouti et al., 2020) disrupts hippocampal synaptic plasticity, hippocampus-dependent memory, and suppresses limbic seizures.

Previous studies have shown that, despite apparently identical E2-induced synaptic potentiation in males and females, multiple signaling components required for initiation of potentiation differ between the sexes. For example, different combinations of estrogen receptors mediate E2's effects in females versus males (Oberlander and Woolley, 2016), and cAMP-regulated protein kinase (PKA) is necessary to initiate E2-induced potentiation in females but not in males (Jain et al., 2019). These observations led to the concept of latent sex differences in which the same endpoint in males and females is achieved through distinct underlying mechanisms in each sex. Whether latent sex differences extend to expression of E2-induced synaptic potentiation is unknown, however. The current study investigated mechanisms that underlie expression of E2-induced synaptic potentiation to determine whether the distinct routes of molecular signaling that are activated by E2 in each sex converge to the same or different effects at the level of postsynaptic AMPA receptors (AMPARs).

By analogy to long-term potentiation (LTP), the postsynaptic component of E2-induced synaptic potentiation likely results from some combination of an increased number of AMPARs at synapses (Isaac et al., 1995; Shi et al., 1999; Andrasfalvy and Magee, 2004; Kopec et al., 2006) and/or an increase in AMPAR conductance (Benke et al., 1998). In turn, increased AMPAR conductance can result from phosphorylation of existing AMPARs (Derkach et al., 1999) and/or replacement of calcium-impermeable AMPARs with calcium-permeable AMPARs (cpAMPARs), which have higher conductance (Swanson et al., 1997) and increase overall synaptic conductance (Benke and Traynelis, 2019).

Several observations indirectly support the idea that cpAMPARs may be involved in E2-induced synaptic potentiation. First, although E2 acutely potentiates both evoked excitatory postsynaptic currents (EPSCs) and spontaneous miniature EPSCs (mEPSCs), the frequency of E2 responsiveness differs between types of experiments. With electrical stimulation to evoke EPSCs, ~60% of recordings in CA1 are E2-responsive (Jain et al., 2019); whereas in mEPSC experiments, only ~45% of recordings respond to E2 (Oberlander and Woolley, 2016). Because synaptic activation is required for cpAMPAR-mediated signaling that leads to stabilization of LTP (Plant et al., 2006), the greater E2 responsiveness of evoked EPSCs suggests involvement of cpAMPARs in E2 potentiation studied with synaptic activation. Second, cpAMPARs are required for PKA-sensitive LTP (Park et al., 2016, 2021) and PKA facilitates surface expression of cpAMPARs (Esteban et al., 2003). That PKA is required for E2-induced synaptic potentiation only in females suggests that cpAMPARs may support E2-induced synaptic potentiation to a greater extent in females than in males.

To investigate these questions, we used electrical stimulation and nonstationary fluctuation analysis (NSFA) of two-photon (2p) evoked unitary EPSCs (2pEPSCs) to study mechanisms underlying expression of E2-induced synaptic potentiation in males and females. The results demonstrated sex differences in the requirement for synaptic activation and involvement of cpAMPARs in E2 potentiation of evoked synaptic currents. In addition, the contribution of increased AMPAR conductance versus nonconductive properties of AMPARs (number of channels × open probability) in the postsynaptic component of E2-induced synaptic potentiation also differed between the sexes. Thus, latent sex differences in the hippocampus extend to expression mechanisms of synaptic potentiation.

Materials and Methods

Animals

Young adult female and male Sprague Dawley rats (50-70 d of age, Envigo) were gonadectomized using aseptic surgical procedures 3–8 d before being used for experiments. All animal procedures were performed in accordance with the National Institutes of Health's Guide for the Care and Use of Laboratory Animals and were approved by the Northwestern University Animal Care and Use Committee.

Preparation of hippocampal slices

Rats were deeply anesthetized with sodium pentobarbital (100-125 mg/kg, i.p.) and transcardially perfused with oxygenated (95% O_2/5% CO_2) ice-cold sucrose-containing artificial cerebrospinal fluid (s-aCSF) containing the following (in mM): 75 NaCl, 25 $NaHCO_3$, 15 dextrose, 75 sucrose, 1.25 NaH_2PO_4, 2 KCl, 2.4 Na pyruvate, 1.3 L-ascorbic acid, 0.5 $CaCl_2$, 3 $MgCl_2$; 305-310 mOsm/L, pH 7.4. The brain was quickly removed, and 300 µm transverse slices through the dorsal hippocampus were cut into a bath of ice-cold s-aCSF using a vibrating tissue slicer (VT1200S, Leica). Slices were incubated at 33°C in oxygenated regular aCSF containing the following (in mM): 126 NaCl, 26 $NaHCO_3$, 10 dextrose, 1.25 NaH_2PO_4, 3 KCl, 2 $CaCl_2$, 1 $MgCl_2$; 305-310 mOsm/L, pH 7.4 for 30 min, then allowed to recover in oxygenated regular aCSF at room temperature for 1-6 h until recording.

Electrophysiological recording

For experiments with electrical stimulation, slices were transferred to a recording chamber mounted on a Zeiss Axioskop and were perfused at a rate of ~2 ml/min with warm (33°C) oxygenated regular aCSF containing the $GABA_A$ and NMDAR blockers, SR-95531 (2 µM) and DL-APV (25 µM), respectively. In 2p experiments, the bath recirculated a small volume (~8 ml) of regular aCSF containing SR-95531 (2 µM), TTX (1 µM), and MNI-glutamate (2 mM). In a subset of experiments, the cpAMPAR blocker, 1-napthyl acetyl spermine (NASPM, 40 µM) (Koike et al., 1997; Park et al., 2016) was bath-applied.

Somatic whole-cell voltage-clamp recordings (V_{hold} = −70 mV) were obtained from visually identified CA1 pyramidal cells using patch electrodes (4-7 MΩ) filled with intracellular solution containing the following (in mM): 115 K-gluconate, 20 KCl, 10 HEPES, 10 Na_2 creatine phosphate, 2 Mg-ATP, 0.3 Na-GTP, and 0.001 QX-314 chloride salt; 285-295 mOsm/L, pH 7.2. A subset of control experiments was performed with Cs-gluconate (115 mM) in place of K-gluconate. In electrical stimulation experiments, a glass bipolar stimulating electrode (10-50 µm tip diameter) filled with regular aCSF was placed in the stratum radiatum 200-250 µm from the recorded cell, and EPSCs were recorded once every 15 s. In 2p experiments, the intracellular solution additionally contained Alexa-594 (20 µM) to visualize dendritic spines. Access resistance and holding current were monitored throughout all recordings, and experiments were terminated if access resistance changed by >20%. Access resistance for 2p glutamate uncaging experiments (n = 29) averaged 25.6 ± 1.3 MΩ, range 15-38 MΩ. All electrophysiology data were acquired with a Multiclamp 700B amplifier and pClamp 10.5 software (Molecular Devices), filtered at 2 kHz, and digitized at 20 kHz using a Digidata 1440A data acquisition system (Molecular Devices).

Two types of experiments with electrical stimulation were performed. In the first, baseline EPSCs were recorded and then stimulation was suspended during 10 min of E2 (100 nM) application and resumed after washing out E2 to investigate whether synaptic activity is required for expression of E2-induced synaptic potentiation. In the second, the cpAMPAR blocker, NASPM, was applied in E2-responsive recordings, either immediately after E2 washout or 10-15 min later.

Two-photon glutamate uncaging

Alexa-594-filled dendritic spines located 57-175 µm from the soma were visualized using a dual galvanometer-based 2p laser scanning system

(Ultima, Prairie Technologies) equipped with a 40× objective with 8-10× digital zoom. Two pulsed laser beams (Chameleon Ultra II, Coherent) were used: one split at 840 nm to image dendritic spines and one at 720 nm to uncage MNI-glutamate at 3-5 spines on one dendrite per recorded cell. Laser beam intensity was controlled with electro-optical modulators (Conoptics, model 350-50) with an uncaging dwell time of 1.0 ms at a laser power (10-50 mW, as measured at the back aperture of the microscope) chosen such that each of 3-5 spines on a dendritic shaft produced 30%-50% of its maximum 2pEPSC amplitude. Uncaging was focused at the edge of targeted spines. Each spine received an uncaging pulse 1-3 times per minute with a 2 s interval between uncaging pulses at different spines. We used 2 or 4 ms uncaging laser pulse widths, which was held constant within an experiment. Control experiments were performed in both sexes to ensure that 2pEPSC amplitude was stable over 30-40 min of recording and was not affected by switching solutions (6 ± 2% from baseline). Under these conditions, 2pEPSC kinetics were comparable to previous studies of 2pEPSCs (Matsuzaki et al., 2001; Harvey and Svoboda, 2007; Lee et al., 2009; Oh et al., 2013) but slower than electrically evoked EPSCs, possibly because of slower dynamics of glutamate uncaged with laser stimulation compared with synaptic release.

Nonstationary fluctuation analysis of two-photon evoked EPSCs

To estimate changes in single-channel properties that underlie postsynaptic expression of E2-induced synaptic potentiation, peak-scaled NSFA was performed on the decay phase of 2pEPSCs according to a published protocol (Hartveit and Veruki, 2007). IGOR-based Neuromatic software was used to align 2pEPSCs based on rise time and to test for stationarity of events based on Spearman rank-order correlation of 2pEPSC amplitude, rise times, and decay times in each condition (baseline and E2) with $p > 0.05$ set as the threshold for stability (Hartveit and Veruki, 2007). This confirmed that both rise time and decay time were stable within each condition. The variance of the fluctuation around the mean EPSC amplitude was calculated in MATLAB for 100 bins of equal current decrement from the peak of the response through three decay time constants, for equivalent sampling across the range of amplitudes during curve fitting. Peak-scaled NSFA was then performed on binned data as follows:

For each dendritic spine in each condition, baseline and E2, the single-channel current (i) and the number of channels (N) were estimated by fitting the data using the theoretical relationship between scaled variance (σ^2) and current amplitude (I) as follows:

$$\sigma^2(I) = iI - \frac{I^2}{N} + \sigma_b^2 \quad (1)$$

where (σ_b^2) is the background variance, (i) is the single-channel current, and (N) is the total number of ion channels available for activation. The single-channel (unitary) chord conductance (γ) can then be calculated as follows:

$$\gamma = i/(V_m - E_{rev}) \quad (2)$$

from the known membrane holding potential ($V_m = -70$ mV) and the estimated AMPAR reversal potential ($E_{rev} = 0$ mV). Because of the low mean open probability of AMPARs, the variance versus mean plot defines only the initial linear phase of the predicted parabola, and therefore does not cover enough arc for extrapolation to the x intercept at a probability of 1, from which N can be estimated. To compensate for this, the events in each condition were scaled to the peak amplitude of the mean EPSC within a condition, as described previously (Traynelis et al., 1993; Hartveit and Veruki, 2007). Estimates of N obtained with peak-scaling reflect the number of AMPAR channels × mean open probability (N*Po). To test whether space clamp errors influenced AMPAR γ estimates in recordings with K-gluconate-based internal solution, we performed a subset of experiments with Cs-gluconate-based internal solution. This showed γ estimates essentially identical to those with K-based internal solution (K-gluconate: 9.2 ± 0.1 pS; Cs-gluconate: 9.4 ± 1.0 pS; $t_{(67)} = 0.15$ $p = 0.87$). Similarly, 2pEPSC decay times did not differ (K-gluconate: 10.9 ± 1.0 ms, Cs-gluconate: 9.6 ± 0.5 ms; $t_{(25)} = 1.23$, $p = 0.22$).

Chemicals

Chemicals were purchased from Tocris BioSciences unless otherwise specified. Stock solutions of DL-APV, SR-95531, NASPM, QX-314, TTX, and Alexa-594 (Invitrogen) were prepared in ddH_2O, while 17β-estradiol (Sigma-Aldrich) was made in DMSO (Sigma-Aldrich). The bath contained an equivalent concentration of DMSO (0.01% v/v) in all phases of each experiment. Stock MNI-glutamate solution was prepared in aCSF. Stock solutions were stored at −20°C and diluted in aCSF on the day of recording to achieve final concentrations.

Experimental design and statistical analyses

Electrical stimulation experiments. To determine the role of synaptic activity in E2-induced synaptic potentiation, stimulation was suspended during 10 min of E2 application. For statistical analysis, experiments were divided into three phases: pre (last 5 min of baseline recording before E2 application), early E2 (first 5 min after stimulation was resumed following E2 washout), and late E2 (last 5 min of the recording). For each recorded cell, ANOVA with multiple comparisons analysis was performed to evaluate differences in EPSC amplitude among pre, early E2, and late E2 phases. This test determined whether a recording was E2-responsive and also whether there was a significant change in EPSC amplitude in the early and/or late E2 phase. Unpaired, two-tailed t tests were performed to determine whether the magnitude of potentiation differed between sexes. Fisher's exact test was used to determine whether the frequency of potentiation differed between sexes. In all cases, $p < 0.05$ was considered to indicate a significant difference. All data from both E2-responsive and -nonresponsive recordings are shown in Figure 1.

To determine the sensitivity of potentiated EPSCs to inhibition of cpAMPARs, individual recordings were first identified as E2-responsive or -nonresponsive using unpaired, two-tailed t tests to compare the amplitudes of EPSCs during the last 5 min of baseline recording to the amplitudes of EPSCs during the first 5 min after E2 washout in each cell. Responsiveness to NASPM was then tested in two ways. First, unpaired, two-tailed t tests were used within each E2-responsive recording to compare EPSC amplitudes during the first 5 min after E2 washout to the last 5 min in NASPM to determine whether an individual recording was responsive to NASPM. Second, overall sensitivity to NASPM was evaluated among all E2-responsive recordings in each sex using paired, two-tailed t tests to compare EPSC amplitude during the first 5 min after E2 washout to the last 5 min in NASPM. In all cases, $p < 0.05$ was considered to indicate a significant difference. All data from both NASPM-responsive and nonresponsive recordings are shown in Figure 2.

Two-photon glutamate uncaging experiments. To determine whether individual dendritic spines were responsive to E2, unpaired, two-tailed t tests were used to compare the amplitudes of 2pEPSCs during the last 5 min of baseline recording to 2pEPSC amplitudes in the same spine during last 5 min after E2 was applied. Unpaired, two-tailed t tests were then used to compare the magnitude of 2pEPSC potentiation in E2-responsive spines in females versus males, and Fisher's exact test was used to determine whether the frequency of E2-responsive spines differed between sexes. In all cases, $p < 0.05$ was considered to indicate a significant difference. All data from E2-responsive and -nonresponsive spines are shown in Figure 3.

Nonstationary fluctuation analysis. The variance versus mean current relationship within each condition (baseline and E2) was determined using Equation 2 as described above. The reliability of the single-channel current (i) was determined using goodness-of-fit r^2 values. Based on previous studies (Matsuzaki et al., 2001; Tanaka et al., 2005) and observations from our analysis, 18 2pEPSCs in each condition was the minimum number to result in a reliable fit with r^2 values of at least 0.6 (range 0.6-0.97) (Banke et al., 2000; Ostertagová, 2012). Therefore, NSFA was performed on the subset of 2pEPSC recordings that had at least 18 events in both baseline and E2 conditions and were stable within each condition.

Peak-scaled NSFA was used to evaluate changes in AMPAR single-channel properties, γ and N*Po, from 2pEPSCs in baseline and E2 conditions. All spines that were determined to be E2-responsive based on a statistically significant change in 2pEPSC amplitude showed at least a 20% change in γ or N*Po, and none of the E2-nonresponsive spines did. Thus, we set 20% as the minimum change to determine E2 responsiveness

of individual spines in NSFA. NSFA results from all E2-responsive and -nonresponsive spines are shown in Figures 4 and 6.

Changes in 2pEPSC 10%-90% rise time and decay time (τ) in E2-responsive and -nonresponsive spines were evaluated statistically using unpaired, two-tailed t tests, shown in Figures 5 and 6. Pearson correlation was to used test for an effect of spine location on γ estimates and to compare changes in decay time and N*Po at individual spines (male and female data were pooled), shown in Figure 5. In all cases, $p < 0.05$ was considered to indicate a significant difference.

Data are presented in the text as mean ± SEM, and results from all individual cells or spines are plotted in the figures. All statistical analyses were performed using Graphpad PRISM software.

Results

Synaptic activity is required for expression of E2-induced synaptic potentiation in females but not in males

Previous experiments have shown that, in both sexes, E2-induced potentiation of synaptically evoked EPSCs begins within 5-8 min when stimulation is continued during E2 application (Jain et al., 2019). To determine whether synaptic activation is required for this potentiation, here, we suspended stimulation specifically while E2 was applied. After recording baseline EPSCs for 10-15 min, stimulation was stopped, E2 was applied for 10 min, then stimulation was resumed beginning 5 min after E2 washout and continued for an additional ≥30 min. Identical experiments were done in females and males.

In females, synaptic activity was required for E2-induced potentiation of EPSCs. There was no change in EPSC amplitude in any of the cells immediately after stimulation was resumed (−2 ± 5% from baseline; Fig. 1*A*,*B*). However, in 7 of 13 cells, EPSC amplitude began to increase with stimulation following E2 washout. By 15-30 min after E2 washout, EPSC amplitude was increased by 74 ± 5% above baseline in these cells (Fig. 1*B*,*C*). The other 6 cells showed no change in EPSC amplitude throughout ≥30 additional minutes of recording (Fig. 1*C*). The frequency and magnitude of E2-induced potentiation by the end of the current experiments in females were similar to E2-induced potentiation with stimulation in females reported previously (83 ± 16% above baseline in 9 of 16 cells) (Jain et al., 2019).

In contrast to females, potentiation of EPSCs in males was apparent immediately upon E2 washout (Fig. 1*D*). In 7 of 15 cells, EPSC amplitude had increased by 95 ± 16% when stimulation was resumed and remained elevated throughout the additional ≥30 min of recording (83 ± 10% above baseline during late E2; Fig. 1*E*,*F*). Neither the magnitude of potentiation (unpaired t test, $t_{(12)} = 0.78$, $p = 0.44$) nor frequency of potentiation (Fisher's exact test, $p > 0.05$) differed between males and females, and E2 responsiveness without stimulation in males was similar to previous experiments in males with stimulation (89 ± 16% above baseline in 11 of 18 cells) (Jain et al., 2019). Like in females, E2-nonresponsive cells in males showed no change in EPSC amplitude throughout recording (Fig. 1*F*). These experiments demonstrate that the requirement for synaptic activation to express E2-induced potentiation is sex-specific.

Sex difference in the requirement of calcium-permeable AMPARs in expression of E2-induced synaptic potentiation

Differential requirement of cpAMPARs to express E2-induced synaptic potentiation could explain the sex difference in its activity dependence. Previous LTP studies have shown that cpAMPARs are transiently incorporated at synapses and that synaptic activation is required for cpAMPAR-mediated signaling to express LTP (Plant et al., 2006). To investigate the requirement of cpAMPARs in E2-induced synaptic potentiation, we used the cpAMPAR blocker NASPM (40 μM). Baseline EPSCs were recorded for 10-15 min and E2 was applied to identify E2-responsive recordings. NASPM was then added either immediately after E2 or 10-15 min later, once potentiated EPSCs had stabilized. Identical experiments were done in females and males.

In females, NASPM applied immediately after E2 application reversed E2-induced EPSC potentiation (Fig. 2*A*), whereas in males NASPM failed to reverse potentiated EPSCs in the majority of cells recorded (Fig. 2*B*). In all 8 E2-responsive cells in females, NASPM decreased potentiated EPSC amplitude within 15-20 min, from 78 ± 13% to 19 ± 8% above baseline (paired t test; E2 vs NASPM, $t_{(7)} = 4.2$, $p = 0.003$; Fig. 2*C*). Within-cell unpaired t tests confirmed that NASPM significantly decreased EPSC amplitude in all 8 female cells (Fig. 2*C*, gray points). In contrast, in males, there was no overall effect of NASPM on potentiated EPSCs. EPSC amplitude was 78 ± 10% above baseline in E2 compared with 56 ± 9% above baseline in NASPM (paired t test; E2 vs NASPM, $t_{(7)} = 2.28$, $p = 0.056$; Fig. 2*D*). This statistical trend was explained by partial reversal of potentiation in 2 of 8 cells in which within-cell unpaired t tests showed that EPSC amplitude was significantly decreased in NASPM compared with E2 (Fig. 2*D*, gray points). NASPM had no effect in the remaining 6 E2-responsive cells in males (Fig. 2*D*, open points). Together, these experiments indicate a sex difference in the role of cpAMPARs in stabilization of E2-induced synaptic potentiation. In females, cpAMPARs are required for stabilization of potentiation, whereas in males, they appear to be involved at a minority of synapses, but potentiation at the majority of male synapses does not require cpAMPARs.

We next tested whether cpAMPARs are required for maintenance of potentiated EPSCs by applying NASPM beginning 10-15 min following E2 washout, after EPSC potentiation had stabilized (Fig. 2*E*). This showed that NASPM had no effect on stabilized potentiation in either females (0 ± 2% change, $n = 6$; Fig. 2*F*) or males (0 ± 3% change, $n = 6$; Fig. 2*G*). Thus, cpAMPARs are not required for ongoing maintenance of E2-induced potentiation in either sex.

Because cpAMPARs have higher conductance compared with other AMPARs (Swanson et al., 1997), it is possible that incorporation of cpAMPARs increases the overall synaptic conductance to potentiate synapses. In addition, calcium influx via cpAMPARs could activate downstream signaling that is required to stabilize potentiation. One way to distinguish between these possibilities is to consider the time required for NASPM to reverse potentiated EPSCs. If NASPM reverses EPSC potentiation solely by blocking current through cpAMPARs, its effect should be rapid, comparable to other AMPAR antagonists, such as DNQX. Alternatively, if NASPM acts by inhibiting cpAMPAR-mediated signaling that is necessary for stabilization of potentiated EPSCs, then it might take longer to reverse potentiated EPSCs. In our experiments, NASPM required at least 15 min to reverse E2-potentiated EPSCs (Fig. 2*A*), which suggests a need for cpAMPAR-mediated signaling to stabilize E2-induced synaptic potentiation, especially in females (in which NASPM was more effective). Consistent with this, at least 15 min of synaptic activity after E2 was required to fully potentiate EPSCs in synaptic activation experiments with females (Fig. 1*A*). Thus, together, these results indicate that females and males differ in their dependence on activity-dependent cpAMPAR signaling for the expression and/or stabilization of E2-induced synaptic potentiation.

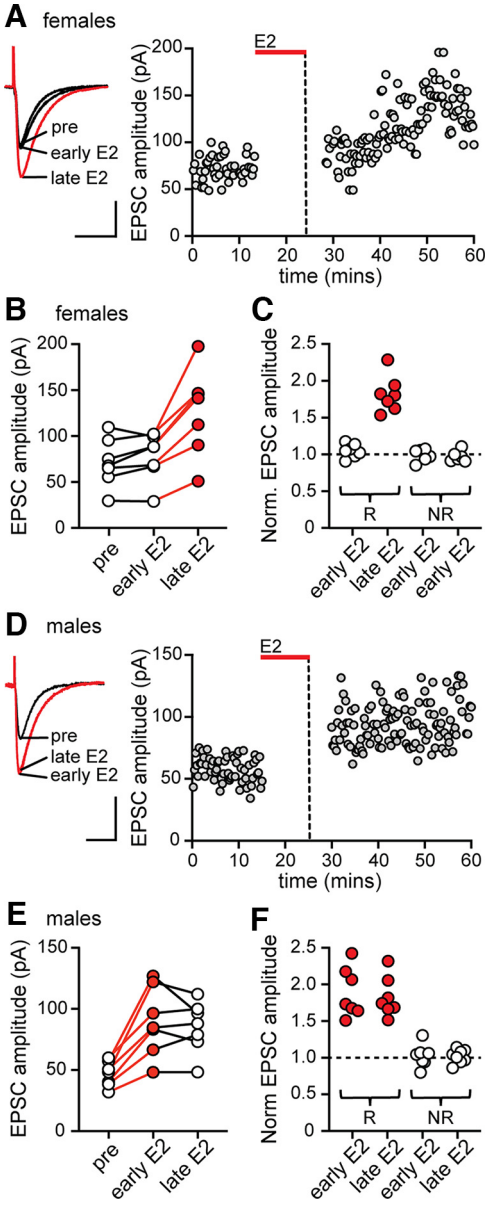

Figure 1. Synaptic activity is required for E2-induced synaptic potentiation in females but not in males. ***A***, Individual traces and time course of synaptic potentiation in a representative experiment in females in which stimulation was suspended during 10 min of E2 application and then resumed 5 min after E2 washout. Early E2 refers to the first 5 min after stimulation was resumed, and late E2 refers to the last 5 min of the recording (also in ***B–F***). Calibration: 50 pA, 25 ms. Each point is an individual sweep (also in ***D***). ***B***, Group EPSC amplitude data in females ($n = 7$) showing that synaptic activity was required to potentiate EPSCs in females. Red points in late E2 indicate a significant increase in EPSC amplitude compared with baseline (within-cell ANOVA followed by multiple comparisons, $p < 0.05$; also in ***C***). ***C***, Normalized EPSC amplitude in E2-responsive (R) and nonresponsive (NR) recordings in the early E2 and late E2 phase of each experiment in females showing that EPSC amplitude was increased only in the late E2 phase. ***D***, Individual traces and time course of synaptic potentiation in a representative experiment in males in which stimulation was suspended during 10 min application of E2 and then resumed 5 min after E2 washout (as in ***A***). ***E***, Group EPSC amplitude data in males ($n = 7$) showing that, in contrast to females, synaptic activity was not required to potentiate EPSCs in males. Red points in early E2 and late E2 indicate a significant difference from baseline (within-cell ANOVA followed by multiple comparisons, $p < 0.05$; also in ***F***). ***F***, Normalized EPSC amplitude in E2-responsive (R) and nonresponsive (NR) recordings in the early E2 and late E2 phase of each experiment in males showing that EPSC amplitude was increased in both phases.

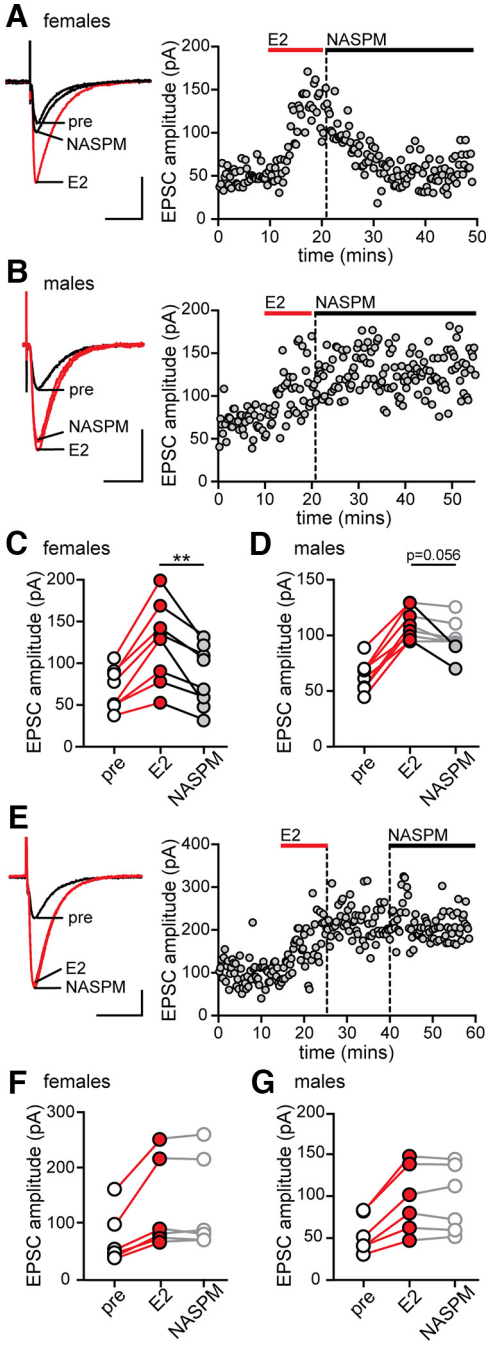

Figure 2. Calcium-permeable AMPARs are required for stabilization of E2-induced synaptic potentiation in females but not in males. ***A***, Individual traces and time course of synaptic potentiation and its reversal by NASPM in a representative experiment in females in which NASPM was applied immediately after E2 washout. Calibration: 50 pA, 25 ms. Each point is an individual sweep (also in ***B***,***E***). ***B***, Individual traces and time course of synaptic potentiation and lack of its reversal by NASPM in a representative experiment in males in which NASPM was applied immediately after E2 washout. ***C***, Group EPSC amplitude data for all E2-responsive recordings in females ($n = 8$). Red points indicate a significant difference from baseline. Gray points indicate a significant effect of NASPM to reverse potentiated EPSCs (within-cell unpaired t tests, $p < 0.05$; also in ***D–G***). $^{**}p < 0.01$, an overall effect of NASPM to decrease EPSC amplitude compared with E2 (paired t test). ***D***, Group EPSC amplitude data for all E2-responsive recordings in males ($n = 8$). NASPM decreased EPSC amplitude in two recordings (gray points) but resulted in only a statistical trend overall (paired t test, $p = 0.056$). ***E***, Individual traces and time course of synaptic potentiation and lack of its reversal in a representative experiment (female) in which NASPM was applied 15 min after E2 washout. ***F***, ***G***, Group EPSC amplitude data for all E2-responsive experiments in females (***F***, $n = 6$) and males (***G***, $n = 6$) in which NASPM was applied 15 min after E2 washout. After stabilization of E2-induced synaptic potentiation, NASPM had no effect in either sex.

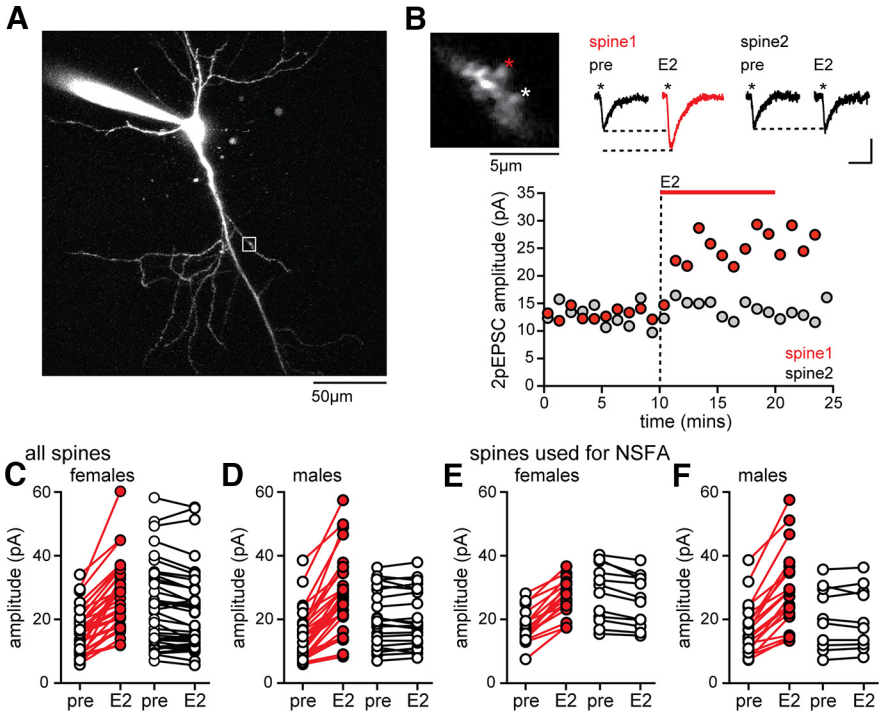

Figure 3. E2 potentiates two-photon evoked EPSCs in a subset of spines in both sexes. ***A***, Representative CA1 pyramidal cell filled with Alexa-594 during recording. White box represents the dendritic segment targeted for 2p glutamate uncaging. ***B***, Higher-magnification view of the dendritic segment indicated in ***A*** showing two spines that were targeted for uncaging (*), individual 2pEPSCs from each spine before (pre) and after E2, and time course of 2pEPSC potentiation in spine 1 (red) but not spine 2 (gray). Calibration: 2pEPSCs, 10 pA, 10 ms. Each point in the time course represents mean 2pEPSC amplitude per minute in each spine. ***C***, Group EPSC amplitude data from all 2pEPSC experiments in females. Red points represent spines in which E2 significantly increased 2pEPSC amplitude (within-spine unpaired *t* tests, $p < 0.05$). White points represent spines in which E2 did not change 2pEPSC amplitude (also in ***D–F***). ***D***, Group EPSC amplitude data from all 2pEPSC experiments in males. ***E***, Group EPSC amplitude data from the subset of spines in ***C*** used to perform NSFA in females. ***F***, Group EPSC amplitude data from the subset of spines in ***D*** used to perform NSFA in males.

Sex difference in AMPAR single-channel properties that underlie expression of postsynaptic E2-induced synaptic potentiation

Results with NASPM indicated that cpAMPAR-mediated signaling plays a role in stabilization of potentiated EPSCs, especially in females. As noted above, it is also possible that cpAMPARs incorporated at synapses result in an overall increase in AMPAR conductance. To investigate mechanisms that underlie the postsynaptic component of E2-induced synaptic potentiation, we evaluated potentiation using 2p-evoked glutamate uncaging. E2 effects at individual synapses were investigated by recording 2pEPSCs from 3-5 spines on one dendritic segment per cell, and E2 was applied for 10 min after recording baseline 2pEPSCs for 10-15 min. Identical experiments were done in females and males.

As has been shown previously (Oberlander and Woolley, 2016), E2 potentiated 2pEPSC amplitude at a subset of spines on the same dendrite (Fig. 3*A*,*B*) in both sexes. Within-spine *t* tests showed that E2 increased 2pEPSC amplitude in 39 of 80 spines from 18 cells in females, by 71 ± 8% (Fig. 3*C*), and in 33 of 54 spines from 12 cells in males, by 91 ± 9% (Fig. 3*D*). With 3-5 spines tested per dendrite, no dendrites in either sex showed all E2-responsive spines, and neither the magnitude of potentiation ($t_{(74)} = 1.43$, $p = 0.15$) nor the frequency of E2 responsiveness (Fisher's exact test, $p > 0.5$) differed between sexes.

A subset of these 2pEPSC recordings met requirements for NSFA in both baseline and E2 conditions (see Materials and Methods). Twenty-nine spines from 9 cells met criteria for analysis in females, of which 17 were E2-responsive (overall 70 ± 7% increase in 2pEPSC amplitude, Fig. 3*E*). Similarly, 30 spines from 8 cells met criteria for analysis in males, of which 20 were responsive to E2 (overall 80 ± 11% increase in 2pEPSC amplitude, Fig. 3*F*).

Using this subset of spines, we then performed NSFA to investigate whether E2-induced potentiation is associated with increased AMPAR γ, N^*Po, or both (Matsuzaki et al., 2001; Tanaka et al., 2005). With this approach, plotting variance in the decay of individual 2pEPSCs versus current amplitude defines a parabola for each condition that can be compared to distinguish changes in γ, indicated by a change in initial slope of the parabola (Fig. 4*A*), from changes in N^*Po, indicated by a change in the size of the parabola with no change in initial slope (Fig. 4*B*).

NSFA indicated that E2-induced potentiation of 2pEPSCs is paralleled by increased AMPAR γ in the majority of spines in females (76%). In 13 of the 17 E2-responsive spines in females, E2 increased γ by 88 ± 16% without changing N^*Po (Fig. 4*C*). In the other four spines, N^*Po was increased, by 330 ± 81%, while γ was either unchanged (2 spines) or strongly decreased (2 spines; Fig. 4*D*). No spines showed both an increase in γ and N^*Po (Fig. 4*E*). In contrast to females, a slight majority of spines in males (60%) was potentiated through an increase in N^*Po with increased γ underlying potentiation in the rest (40%). E2 increased γ, by 122 ± 19%, in 8 of 20 E2-responsive spines in males with no change in N^*Po (Fig. 4*F*). The other 12 male spines showed a 136 ± 27% increase in N^*Po with no change in γ (Fig. 4*G*,*H*). The difference in proportions of spines showing potentiation via increased AMPAR γ versus N^*Po in females compared with males was statistically significant (Fisher's exact test $p < 0.05$), demonstrating a sex difference in AMPAR modulation that underlies postsynaptic potentiation by E2. In addition, these experiments showed that E2 potentiation of spines on the same dendrite can occur through distinct mechanisms. Three dendrites in females and two dendrites in males had spines in which E2 increased γ in one spine and N^*Po in another indicating that different postsynaptic signaling mechanisms can operate to increase synapse strength in nearby spines simultaneously. Finally, as expected, NSFA on spines in which E2 did not potentiate 2pEPSC amplitude showed no changes in either γ or N^*Po in either sex (Fig. 4*I–K*). In addition, and consistent with previous studies (Benke et al., 2001), there was no relationship between the distance of a spine from the soma and γ estimates considering all spines ($r^2 = 0.001$, $p = 0.83$), spines that showed an E2-induced increase in γ ($r^2 = 0.006$, $p = 0.73$), or spines that showed an E2-induced increase in N^*Po ($r^2 = 0.02$, $p = 0.6$).

We also tested whether E2 affects 2pEPSC kinetics and whether 2pEPSC kinetics correlate with changes in single-channel parameters. This showed that, while 2pEPSC rise time was unaffected by E2 in any spines, 2pEPSC decay time was increased

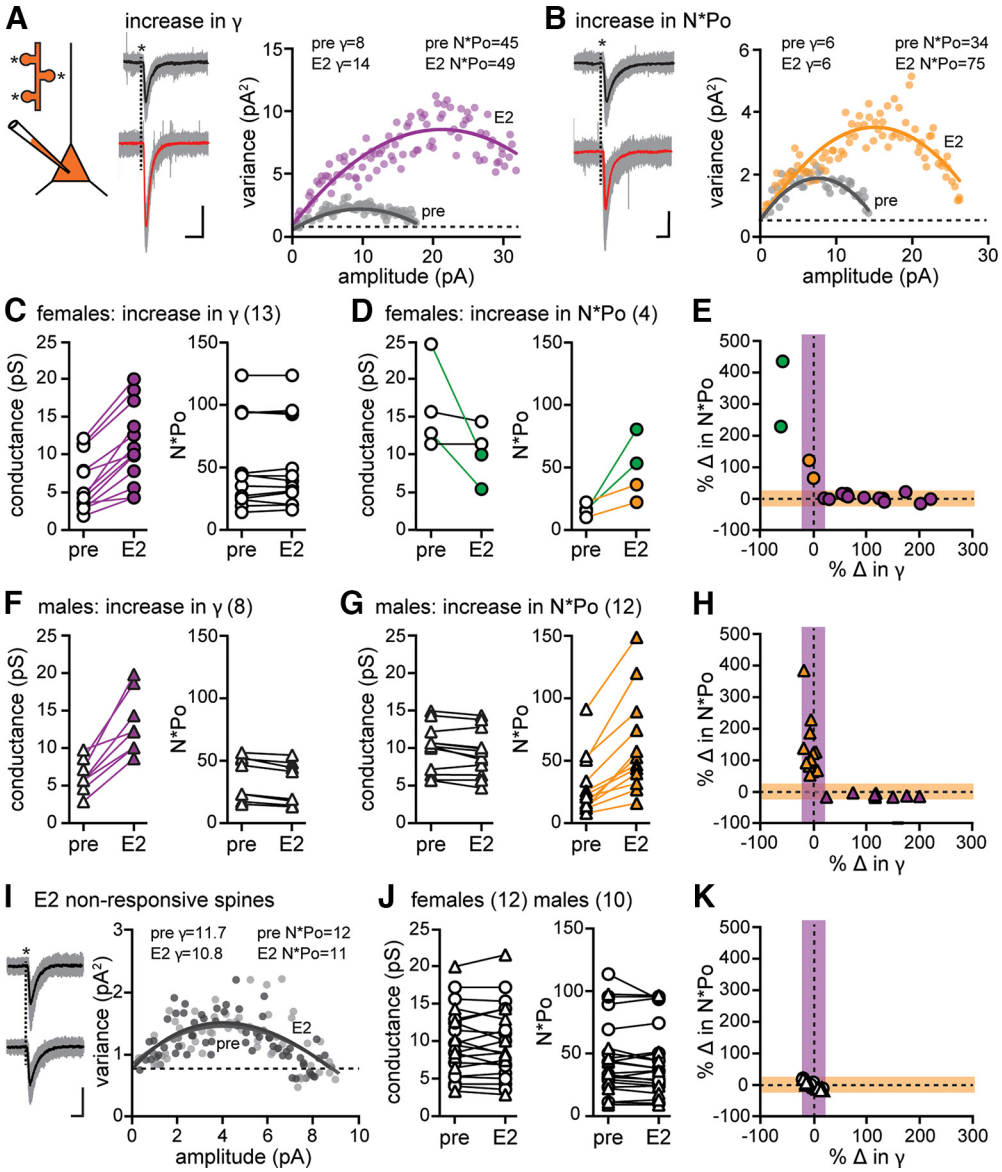

Figure 4. Nonstationary fluctuation analysis indicates a sex difference in AMPAR modulation that underlies expression of E2-induced synaptic potentiation. ***A***, Glutamate was uncaged (*) at multiple dendritic spines on a dendrite of each recorded cell. Data are from a representative female spine in which E2 increased 2pEPSC amplitude and AMPAR conductance (γ), but not number × mean open probability (*N**Po). Traces represent all 2pEPSCs (22 events, gray) and mean (black) during baseline and all 2pEPSCs (25 events, gray) and mean (red) after E2. Calibration: ***A***, ***B***, 5 pA, 5 ms. The variance versus mean plot for this spine indicated that E2 (purple) increased γ compared with baseline (pre, gray) with no change in *N**Po. The goodness-of-fit R^2 values for these plots are 0.92 (pre) and 0.82 (E2). Dotted line indicates the background variance (also in ***B***,***I***). ***B***, Data are from a representative male spine in which E2 increased 2pEPSC amplitude and *N**Po, but not conductance. Traces represent all 2pEPSCs (19 events, gray) and mean (black) during baseline and all 2pEPSCs (33 events, gray) and mean (red) after E2. The variance versus mean plot for this spine indicated that E2 (gold) increased *N**Po compared with baseline (pre, gray) with no change in conductance. The goodness-of-fit R^2 values for these plots are 0.88 (pre) and 0.85 (E2). ***C***, Group conductance and *N**Po estimates in females obtained by NSFA in E2-responsive spines that showed increased conductance (purple) compared with baseline ($n = 13$) with no change in *N**Po in the same spines. ***D***, Group conductance and *N**Po estimates in females obtained by NSFA in E2-responsive spines that showed increased *N**Po compared with baseline ($n = 4$) with no increase in conductance. Two of these spines showed no change in conductance (open), and two showed a decrease (green). ***E***, Normalized changes in *N**Po versus conductance for the same E2-responsive spines in females shown in ***C*** and ***D*** ($n = 17$), where shaded regions represent the 20% threshold for a change in either property (also in ***H***,***K***). ***F***, Group conductance and *N**Po estimates in males obtained by NSFA in E2-responsive spines that showed increased conductance (purple) compared with baseline ($n = 8$) with no change in *N**Po. ***G***, Group conductance and *N**Po estimates in males obtained by NSFA in E2-responsive spines that showed increased *N**Po compared with baseline ($n = 12$) with no change in conductance. The fraction of E2-responsive spines showing an increase in conductance was significantly greater in females than males (Fisher's exact test, $p < 0.05$). ***H***, Normalized changes in *N**Po versus conductance for the same E2-responsive spines in males shown in ***F*** and ***G*** ($n = 20$). ***I***, Data are from a representative spine in which E2 did not change EPSC amplitude. Traces represent all 2pEPSCs (26 events, gray) and mean (black) during baseline and all 2pEPSCs (20 events, gray) and mean (black) after E2. The variance versus mean plot for this spine indicated that E2 (dark gray) affected neither conductance nor *N**Po compared with baseline (pre, light gray). The goodness-of-fit R^2 values for these plots are 0.88 (pre) and 0.90 (E2). ***J***, Group conductance and *N**Po measurements obtained by NSFA in all E2-nonresponsive spines ($n = 12$ females, $n = 10$ males), showing no changes in either property. ***K***, Normalized change in *N**Po versus conductance for the same E2-nonresponsive spines shown in ***J*** ($n = 12$ females, $n = 10$ males).

specifically in E2-responsive spines (unpaired *t* test, $t_{(72)} = 2.18$, $p = 0.03$; Fig. 5*A*,*B*). Interestingly, among E2-responsive spines, the increase in decay time showed a weak but statistically significant correlation with the increase in *N**Po (Pearson correlation, $r^2 = 0.33$, $p = 0.003$; Fig. 5*C*). This was true for both females and males where the majority of spines that showed an increase in decay time also showed an increase in *N**Po (Fig. 5*D*). This parallels a similar relationship shown previously for LTP in

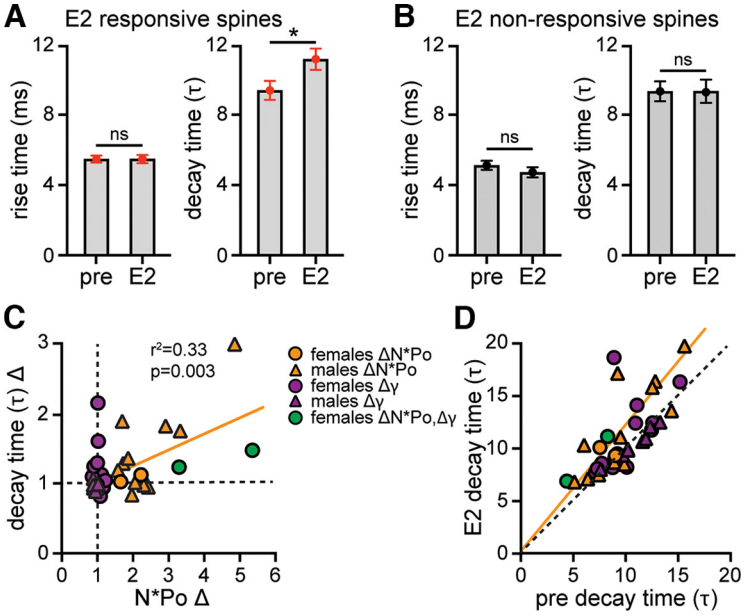

Figure 5. Relationship between E2 modulation of 2pEPSC kinetics and AMPAR single-channel properties. ***A***, Mean ± SEM 2pEPSC rise time and decay time (τ) in the same E2-responsive spines shown in Figure 4. ***B***, Mean ± SEM 2pEPSC rise time and decay time (τ) in the same E2-nonresponsive spines shown in Figure 4. E2 increased decay time specifically in E2-responsive spines but did not affect rise time in any spines. $^*p < 0.05$ (unpaired *t* test). ***C***, Comparison of fold-change in decay time (τ) versus AMPAR number × mean open probability (*N**Po) among all E2-responsive spines showing a statistically significant correlation ($r^2 = 0.33$, $p = 0.003$). ***D***, Comparison of decay time (τ) in E2 versus baseline (pre) conditions among all E2-responsive spines using linear regression analysis showing that the majority of spines in which decay time increased also showed an increase in *N**Po (orange and green). Orange line indicates the fitting for spines that show an increase in *N**Po, which is different from the perfect linear fit (black dashed line, $p < 0.001$, simple linear regression).

which increased AMPAR current decay time corresponded to an increase in *N* with no change in Po (or γ) (Andrasfalvy and Magee, 2004).

Calcium-permeable AMPARs are required for the E2-induced increase in AMPAR conductance

To investigate a link between cpAMPARs and E2-induced changes in γ indicated by NSFA, we repeated NSFA of 2pEPSCs in the presence of NASPM (40 μM). As before, 2pEPSCs were recorded from 3-5 spines on one dendritic segment per cell and E2 was applied for 10 min following 10-15 min of baseline recording. Identical experiments were done in females and males. Baseline 2pEPSC amplitude (15.4 ± 1.3 pA) and AMPAR conductance (11.8 ± 0.8 pS) in NASPM were similar to control conditions (16.7 ± 1.3 pA, 9.2 ± 0.1 pS), indicating little, if any, contribution of cpAMPARs to baseline EPSCs, as has been shown previously (Plant et al., 2006).

In females, E2 failed to potentiate 2pEPSCs in any of 23 spines recorded from 6 cells in the presence of NASPM (−10 ± 6% from baseline). In contrast, in males, E2 did potentiate 2pEPSCs in NASPM (Fig. 6*A–C*), but less often than in control conditions. Of 24 spines recorded from 5 male cells, E2 potentiated EPSC amplitude in 7 spines, by 51 ± 13%. This frequency of 2pEPSC potentiation in NASPM (29% of spines) was significantly lower than in control conditions (61% of spines, Fig. 3; Fisher's exact test, $p < 0.05$), raising the possibility that inhibiting cpAMPARs eliminated potentiation at spines that otherwise would have potentiated via increased γ leaving potentiation at spines that potentiate via increased *N**Po intact.

To test this, we performed NSFA on all recordings that met criteria for analysis ($n = 6$ E2-responsive male spines, $n = 10$ nonresponsive male spines, $n = 16$ nonresponsive female spines). In the 6 male spines in which E2 potentiated 2pEPSC amplitude in NASPM, NSFA showed an 81 ± 16% increase in *N**Po with no change in γ at any spines (Fig. 6*D–F*). As expected, there were no changes in AMPAR properties in the E2-nonresponsive spines of either sex (Fig. 6*G–I*). Consistent with results in control conditions, 2pEPSC rise time was not affected by E2, but decay time increased specifically in the subset of spines that potentiated (unpaired *t* test, $t_{(10)} = 2.19$, $p = 0.043$, Fig. 6*J–L*). These results confirmed that the postsynaptic component of E2-induced synaptic potentiation is entirely dependent on cpAMPARs in females but only partly dependent on cpAMPARs in males. In addition, cpAMPARs are necessary for E2-induced potentiation that occurs through increased γ but not for potentiation that occurs through increased *N**Po.

Discussion

In this study, we demonstrate sex differences in the mechanisms that underlie expression of E2-induced synaptic potentiation in the hippocampus. In females, expression of potentiation was activity-dependent and its stabilization required cpAMPARs, whereas in males, neither synaptic activity nor cpAMPARs were required. These differences were paralleled by a sex difference in modulation of AMPAR channel properties that underlie the postsynaptic component of potentiation. NSFA showed that most synapses in females were potentiated via increased AMPAR conductance with no change in nonconductive properties, whereas in males, a slight majority of potentiated synapses showed an increase in nonconductive properties with no change in conductance. Potentiation via increased conductance required cpAMPARs in both sexes. These results demonstrate that the distinct molecular signaling activated by E2 to initiate synaptic potentiation in each sex (Oberlander and Woolley, 2016; Jain et al., 2019) does not converge to a common mechanism of expression, but rather, leads to different patterns of AMPAR modulation that produce apparently identical synaptic potentiation measured electrophysiologically. In this way, the current results extend the concept of latent sex differences in which the same outcome in males and females is achieved through different underlying mechanisms.

Interpretation of nonstationary fluctuation analysis to study expression mechanisms of E2-induced synaptic potentiation

NSFA of 2pEPSCs evoked by glutamate uncaging has two main advantages for studying postsynaptic mechanisms that underlie synaptic potentiation. First, mechanisms operating at individual, identified synapses can be studied without the potential confound of changes in presynaptic neurotransmitter release, and second, it allows estimation of single-channel properties when direct single-channel recordings are not feasible, such as at dendritic spine synapses. Plotting variance in the decay of individual EPSCs versus current amplitude yields data that theoretically should define a parabola (Sigworth, 1980; Benke et al., 2001; Hartveit and Veruki, 2007). When mean open probability of

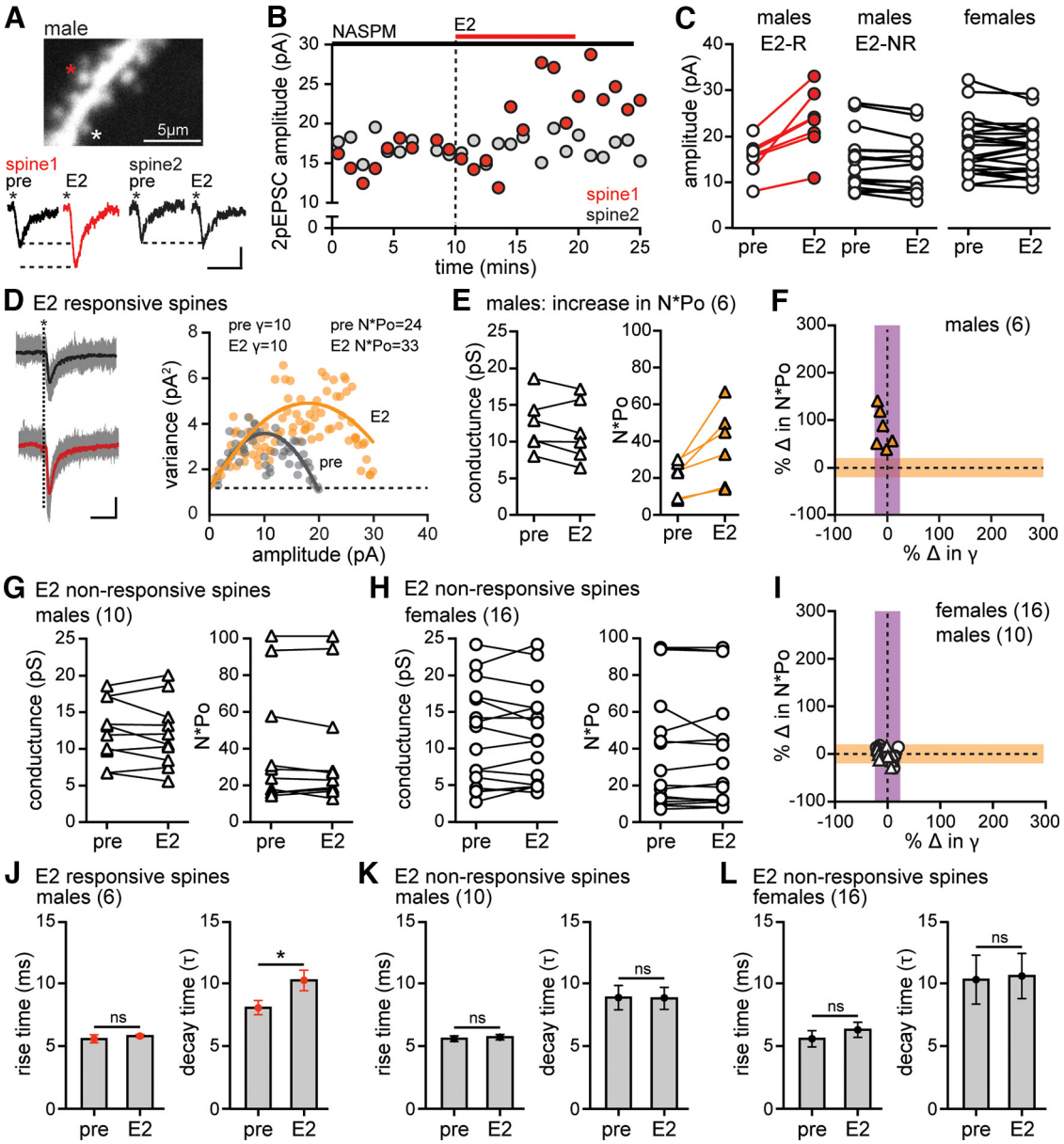

Figure 6. cpAMPARs are required for the E2-induced increase in AMPAR conductance. ***A***, High-magnification view of a dendritic segment from a cell (male) filled with Alexa-594 during recording in NASPM showing two dendritic spines that were targeted for uncaging (*) and individual 2pEPSCs from each spine before (pre) and after E2. Calibration: 5 pA, 5 ms. ***B***, Time course of 2pEPSC potentiation in spine 1 (red) but not spine 2 (gray) for the same spines shown in ***A***. ***C***, Group 2pEPSC amplitude data for all E2-responsive (E2-R, red) and nonresponsive (E2-NR, white) spines recorded in NASPM, showing potentiation in a subset of spines in males ($n = 7$), whereas other spines in males ($n = 10$) and all spines in females ($n = 16$) were E2-nonresponsive. ***D***, 2pEPSC traces and variance versus mean plot for a representative male spine in which E2 increased 2pEPSC amplitude and AMPAR number × mean open probability (*N**Po) with no change in conductance (γ). Traces represent all 2pEPSCs (18 events, gray) and mean (black) during baseline and all 2pEPSCs (23 events, gray) and mean (red) after E2. Calibration: 5 pA, 5 ms. The goodness-of-fit R^2 values for these plots are 0.79 (pre, gray) and 0.86 (E2, gold). Dotted line indicates the background variance. ***E***, Group data showing conductance and *N**Po estimates obtained by NSFA in the 6 male spines that showed E2-induced 2pEPSC potentiation in NASPM and met criteria for analysis. ***F***, Normalized changes in *N**Po versus conductance from NSFA in all E2-responsive male spines shown in ***E*** in which the shaded areas represent the 20% threshold for a change in either property. All 6 E2-responsive male spines recorded in NASPM showed increased *N**Po (orange triangles) with no change in conductance. ***G***, Group data showing no changes in conductance or *N**Po estimates obtained by NSFA in the 10 E2-nonresponsive male spines. ***H***, Group data showing no changes in conductance or *N**Po estimates obtained by NSFA in any of the 16 E2-nonresponsive female spines. ***I***, Normalized changes in *N**Po versus conductance from NSFA in all E2-nonresponsive spines in NASPM ($n = 16$ females, $n = 10$ males). ***J***, Mean ± SEM 2pEPSC rise time and decay time (τ) in E2-responsive male spines recorded in NASPM showing that E2 increased in decay time specifically in E2-responsive spines in males (*$p < 0.05$, unpaired *t* test) with no change in rise time in any of the spines. ***K***, ***L***, Mean ± SEM 2pEPSC rise time and decay time in E2-nonresponsive male (***K***) and female (***L***) spines recorded in NASPM showing no changes (unpaired *t* test).

channels is low, however, as for AMPARs in CA1 dendritic spine synapses (Matsuzaki et al., 2001), most of the data fall in the initial linear portion of the parabola, precluding estimates of *N* from conventional NSFA. Thus, to obtain estimates of both conductive and nonconductive properties that could be compared before and after E2, we performed peak-scaled NSFA. One caveat of this approach is that, because peak-scaling artificially increases mean open probability to 1, changes in *N* cannot be distinguished from changes in Po in our experiments. That said, the observation that 2pEPSC decay time increased specifically in E2-potentiated spines suggests that E2-induced increases in *N**Po are driven by an increase in *N* rather than Po. A previous study using conventional NSFA on AMPAR currents evoked by focal glutamate application to outside-out membrane patches with

and without LTP induction showed that increased AMPAR current decay time corresponds to an increase in N with no change in Po (or γ) (Andrasfalvy and Magee, 2004). Despite this precedent, we cannot rule out the possibilities that E2 increases Po at some synapses or that longer 2pEPSC decay in E2-responsive spines reflects increased AMPAR channel open time.

Our estimates of conductance ranged from 3 to 24 pS, comparable to that expected from single-channel recordings (Rosenmund et al., 1998) but with an upper range higher than previously reported for synapses in the hippocampus (Watson et al., 2017; Park et al., 2021). It is possible that the slower dynamics of uncaged glutamate resulted in overestimates of conductance, which is a limitation. However, because we used peak-scaled NSFA (Traynelis et al., 1993), which is less sensitive than conventional NSFA to variance from factors other than stochastic channel gating, and compared 2pEPSCs at the same spines before and after E2, this is unlikely to have affected our conclusions. Furthermore, there was no relationship between conductance and the distance of a spine from the recording electrode at the soma, no difference in conductance estimates using K-based or Cs-based internal solution, and E2 increased conductance estimated from some spines on a dendrite with no effect on conductance at neighboring spines on the same dendrite in the same recording. Thus, the E2-induced increases in conductance indicated by NSFA in our experiments most likely reflect AMPAR modulation that underlies 2pEPSC potentiation rather than technical artifacts.

The finding that E2 potentiation of 2pEPSCs corresponded either to increased conductance or increased nonconductive properties, and never both, shows that there are distinct mechanisms by which E2-induced synaptic potentiation is expressed at different synapses. The frequency of these mechanisms differs between the sexes, with increased conductance predominating in females. Interestingly, however, we found in both sexes that both mechanisms could operate simultaneously at different spines on the same dendrite.

Sex difference in the requirement of calcium-permeable AMPARs in E2-induced synaptic potentiation

The sex difference in prevalence of an E2-induced increase in AMPAR conductance versus nonconductive properties likely arises from differences in the molecular signaling activated by E2 in each sex. The cpAMPAR inhibitor NASPM required at least 15 min to reverse E2-induced synaptic potentiation and produced much stronger reversal of potentiation in females than males, indicating that female synapses are more reliant on cpAMPARs during stabilization of potentiation than male synapses are. In addition, synaptic activity was required to express potentiation only in females. Both these sex differences indicate that cpAMPAR signaling, likely calcium influx, plays a greater role in E2-induced synaptic potentiation in females than in males. Notably, the requirement for cpAMPARs in females was transient in that with ~15 additional mins of synaptic stimulation after E2, synapses were no longer sensitive to NASPM. In this way, E2-induced synaptic potentiation in females resembles the transient dependence of pairing-induced LTP on cpAMPARs reported by Plant et al. (2006).

It is interesting to note that, whereas inhibition of cpAMPARs had very little effect on E2 potentiation of synaptically evoked EPSCs in males, 2p experiments indicated that a fraction of male synapses (those that potentiated via increased AMPAR conductance) is sensitive to cpAMPAR inhibition. One possibility to explain this apparent discrepancy is that male synapses may have both cpAMPAR-dependent and cpAMPAR-independent routes to downstream signaling required to support E2 potentiation, whereas female synapses have only cpAMPAR-dependent routes; cpAMPAR-independent pathway(s) appear to be sufficient to support potentiation in males when cpAMPARs are blocked.

The requirement for cpAMPARs in E2-induced synaptic potentiation in females may also be related to our previous observation that initiation of potentiation by E2 requires PKA only in females (Jain et al., 2019). For example, PKA-dependent LTP involves insertion of cpAMPARs and results in an increase in single-channel conductance (Park et al., 2021), whereas PKA-independent LTP does not require cpAMPARs (Park et al., 2016). E2 regulation of PKA in females could promote surface localization of AMPARs, including cpAMPARs, by phosphorylating S845 of GluA1 (Oh et al., 2006; Man et al., 2007), which is a necessary step for synaptic incorporation of GluA1-containing AMPARs in LTP (Esteban et al., 2003).

Both cpAMPAR-dependent and -independent pathways likely lead to activation of CaMKII. Previously, we found that CaMKII is required for expression and ongoing maintenance of E2-induced synaptic potentiation in both sexes (Jain et al., 2019). In females, calcium influx through cpAMPARs could increase AMPAR conductance via CaMKII-dependent phosphorylation of GluA1 S831 (Derkach et al., 1999; Poncer et al., 2002; Kristensen et al., 2011) and/or it could activate CaMKII to phosphorylate stargazin, leading to diffusional trapping of GluA1 (and/or GluA2)-containing AMPARs at synapses (Opazo et al., 2010). As suggested above, these mechanisms also could operate in males when cpAMPARs are available. However, when cpAMPARs are blocked, an alternative source of calcium, such as calcium release from internal stores, could activate CaMKII in males. For example, calcium release from internal stores has been shown to activate CaMKII and promote its interaction with PICK1 to increase surface expression of GluA2-containing AMPARs (Lu et al., 2014). The possibility that parallel and compensatory calcium sources can support expression of E2 potentiation in males mirrors our previous finding of similar parallel and compensatory calcium sources for initiation of E2 potentiation in males (Jain et al., 2019). Additional experiments will be needed to dissect distinct calcium signaling mechanisms that underlie the expression of E2 potentiation in each sex.

Implications of latent sex differences in expression of synaptic potentiation

Acute E2-induced synaptic potentiation is a useful model to understand how estrogens synthesized in the brain influence hippocampus-dependent learning and memory (Lu et al., 2019) and seizure activity (Sato and Woolley, 2016). Our laboratory and others are actively pursuing these questions. Moreover, recognition of latent sex differences in mechanisms by which E2 produces equivalent synaptic potentiation in each sex can also provide insight into mechanisms of synaptic plasticity more generally. For example, the PKA dependence of E2-induced synaptic potentiation in females led us to discover that the widely reported PKA independence of early LTP (e.g., Huang and Kandel, 1994; Abel et al., 1997) is true only in males (Jain et al., 2019). Similarly, the sex-dependent role for cpAMPARs in E2-induced synaptic potentiation revealed in the current study may inform a debate about involvement of cpAMPARs in LTP. Whereas Plant et al. (2006) found that transient incorporation of cpAMPARs is required for pairing-induced LTP, another group failed to replicate this (Adesnik and Nicoll, 2007). Explanations for the disparity have been suggested (Park et al., 2016), including differential stress (Whitehead et al., 2013). Our results demonstrate that

the sex of animals used can also contribute to different outcomes in otherwise comparable experiments. Given that mechanistic analyses of synaptic plasticity and other types of neuromodulation provide a pipeline of new information and ideas to inform the development of novel therapeutics, the existence of latent sex differences in mechanisms of synaptic plasticity indicates that results derived from experiments in one sex cannot be assumed to apply to both.

References

Abel T, Nguyen PV, Barad M, Deuel TA, Kandel ER, Bourtchouladze R (1997) Genetic demonstration of a role for PKA in the late phase of LTP and in hippocampus-based long-term memory. Cell 88:615–626.

Adesnik H, Nicoll RA (2007) Conservation of glutamate receptor 2-containing AMPA receptors during long-term potentiation. J Neurosci 27:4598–4602.

Andrasfalvy BK, Magee JC (2004) Changes in AMPA receptor currents following LTP induction on rat CA1 pyramidal neurones. J Physiol 559:543–554.

Banke TG, Bowie D, Lee H, Huganir RL, Schousboe A, Traynelis SF (2000) Control of GluR1 AMPA receptor function by cAMP-dependent protein kinase. J Neurosci 20:89–102.

Benke T, Traynelis SF (2019) AMPA-type glutamate receptor conductance changes and plasticity: still a lot of noise. Neurochem Res 44:539–548.

Benke TA, Luthi A, Isaac JT, Collingridge GL (1998) Modulation of AMPA receptor unitary conductance by synaptic activity. Nature 393:793–797.

Benke TA, Luthi A, Palmer MJ, Wikstrom MA, Anderson WW, Isaac JT, Collingridge GL (2001) Mathematical modelling of nonstationary fluctuation analysis for studying channel properties of synaptic AMPA receptors. J Physiol 537:407–420.

Derkach V, Barria A, Soderling TR (1999) Ca^{2+}/calmodulin-kinase II enhances channel conductance of alpha-amino-3-hydroxy-5-methyl-4-isoxazolepropionate type glutamate receptors. Proc Natl Acad Sci USA 96:3269–3274.

Esteban JA, Shi SH, Wilson C, Nuriya M, Huganir RL, Malinow R (2003) PKA phosphorylation of AMPA receptor subunits controls synaptic trafficking underlying plasticity. Nat Neurosci 6:136–143.

Hartveit E, Veruki ML (2007) Studying properties of neurotransmitter receptors by nonstationary noise analysis of spontaneous postsynaptic currents and agonist-evoked responses in outside-out patches. Nat Protoc 2:434–448.

Harvey CD, Svoboda K (2007) Locally dynamic synaptic learning rules in pyramidal neuron dendrites. Nature 450:1195–1200.

Hojo Y, Hattori TA, Enami T, Furukawa A, Suzuki K, Ishii HT, Mukai H, Morrison JH, Janssen WG, Kominami S, Harada N, Kimoto T, Kawato S (2004) Adult male rat hippocampus synthesizes estradiol from pregnenolone by cytochromes P45017alpha and P450 aromatase localized in neurons. Proc Natl Acad Sci USA 101:865–870.

Hojo Y, Higo S, Ishii H, Ooishi Y, Mukai H, Murakami G, Kominami T, Kimoto T, Honma S, Poirier D, Kawato S (2009) Comparison between hippocampus-synthesized and circulation-derived sex steroids in the hippocampus. Endocrinology 150:5106–5112.

Huang GZ, Woolley CS (2012) Estradiol acutely suppresses inhibition in the hippocampus through a sex-specific endocannabinoid and mGluR-dependent mechanism. Neuron 74:801–808.

Huang YY, Kandel ER (1994) Recruitment of long-lasting and protein kinase A-dependent long-term potentiation in the CA1 region of hippocampus requires repeated tetanization. Learn Mem 1:74–82.

Isaac JT, Nicoll RA, Malenka RC (1995) Evidence for silent synapses: implications for the expression of LTP. Neuron 15:427–434.

Jain A, Huang GZ, Woolley CS (2019) Latent sex differences in molecular signaling that underlies excitatory synaptic potentiation in the hippocampus. J Neurosci 39:1552–1565.

Koike M, Iino M, Ozawa S (1997) Blocking effect of 1-naphthyl acetyl spermine on Ca(2+)-permeable AMPA receptors in cultured rat hippocampal neurons. Neurosci Res 29:27–36.

Kopec CD, Li B, Wei W, Boehm J, Malinow R (2006) Glutamate receptor exocytosis and spine enlargement during chemically induced long-term potentiation. J Neurosci 26:2000–2009.

Kramar EA, Chen LY, Brandon NJ, Rex CS, Liu F, Gall CM, Lynch G (2009) Cytoskeletal changes underlie estrogen's acute effects on synaptic transmission and plasticity. J Neurosci 29:12982–12993.

Kristensen AS, Jenkins MA, Banke TG, Schousboe A, Makino Y, Johnson RC, Huganir R, Traynelis SF (2011) Mechanism of Ca^{2+}/calmodulin-dependent kinase II regulation of AMPA receptor gating. Nat Neurosci 14:727–735.

Lee SJ, Escobedo-Lozoya Y, Szatmari EM, Yasuda R (2009) Activation of CaMKII in single dendritic spines during long-term potentiation. Nature 458:299–304.

Lu W, Khatri L, Ziff EB (2014) Trafficking of alpha-amino-3-hydroxy-5-methyl-4-isoxazolepropionic acid receptor (AMPA) receptor subunit GluA2 from the endoplasmic reticulum is stimulated by a complex containing Ca^{2+}/calmodulin-activated kinase II (CaMKII) and PICK1 protein and by release of Ca^{2+} from internal stores. J Biol Chem 289:19218–19230.

Lu Y, Sareddy GR, Wang J, Wang R, Li Y, Dong Y, Zhang Q, Liu J, O'Connor JC, Xu J, Vadlamudi RK, Brann DW (2019) Neuron-derived estrogen regulates synaptic plasticity and memory. J Neurosci 39:2792–2809.

Man HY, Sekine-Aizawa Y, Huganir RL (2007) Regulation of α-amino-3-hydroxy-5-methyl-4-isoxazolepropionic acid receptor trafficking through PKA phosphorylation of the Glu receptor 1 subunit. Proc Natl Acad Sci USA 104:3579–3584.

Marbouti L, Zahmatkesh M, Riahi E, Sadr SS (2020) Inhibition of brain 17beta-estradiol synthesis by letrozole induces cognitive decline in male and female rats. Neurobiol Learn Mem 175:107300.

Matsuzaki M, Ellis-Davies GC, Nemoto T, Miyashita Y, Iino M, Kasai H (2001) Dendritic spine geometry is critical for AMPA receptor expression in hippocampal CA1 pyramidal neurons. Nat Neurosci 4:1086–1092.

Oberlander JG, Woolley CS (2016) 17β-estradiol acutely potentiates glutamatergic synaptic transmission in the hippocampus through distinct mechanisms in males and females. J Neurosci 36:2677–2690.

Oh MC, Derkach VA, Guire ES, Soderling TR (2006) Extrasynaptic membrane trafficking regulated by GluR1 serine 845 phosphorylation primes AMPA receptors for long-term potentiation. J Biol Chem 281:752–758.

Oh WC, Hill TC, Zito K (2013) Synapse-specific and size-dependent mechanisms of spine structural plasticity accompanying synaptic weakening. Proc Natl Acad Sci USA 110:E305–E312.

Opazo P, Labrecque S, Tigaret CM, Frouin A, Wiseman PW, De Koninck P, Choquet D (2010) CaMKII triggers the diffusional trapping of surface AMPARs through phosphorylation of stargazin. Neuron 67:239–252.

Ostertagová E (2012) Modelling using polynomial regression. Proc Eng 48:500–506.

Park P, Sanderson TM, Amici M, Choi SL, Bortolotto ZA, Zhuo M, Kaang BK, Collingridge GL (2016) Calcium-permeable AMPA receptors mediate the induction of the protein kinase A-dependent component of long-term potentiation in the hippocampus. J Neurosci 36:622–631.

Park P, Georgiou J, Sanderson TM, Ko KH, Kang H, Kim JI, Bradley CA, Bortolotto ZA, Zhuo M, Kaang BK, Collingridge GL (2021) PKA drives an increase in AMPA receptor unitary conductance during LTP in the hippocampus. Nat Commun 12:413.

Plant K, Pelkey KA, Bortolotto ZA, Morita D, Terashima A, McBain CJ, Collingridge GL, Isaac JT (2006) Transient incorporation of native GluR2-lacking AMPA receptors during hippocampal long-term potentiation. Nat Neurosci 9:602–604.

Poncer JC, Esteban JA, Malinow R (2002) Multiple mechanisms for the potentiation of AMPA receptor-mediated transmission by alpha-Ca^{2+}/calmodulin-dependent protein kinase II. J Neurosci 22:4406–4411.

Rosenmund C, Stern-Bach Y, Stevens CF (1998) The tetrameric structure of a glutamate receptor channel. Science 280:1596–1599.

Sato SM, Woolley CS (2016) Acute inhibition of neurosteroid estrogen synthesis suppresses status epilepticus in an animal model. Elife 5:e12917.

Shi SH, Hayashi Y, Petralia RS, Zaman SH, Wenthold RJ, Svoboda K, Malinow R (1999) Rapid spine delivery and redistribution of AMPA receptors after synaptic NMDA receptor activation. Science 284:1811–1816.

Sigworth FJ (1980) The conductance of sodium channels under conditions of reduced current at the node of Ranvier. J Physiol 307:131–142.

Smejkalova T, Woolley CS (2010) Estradiol acutely potentiates hippocampal excitatory synaptic transmission through a presynaptic mechanism. J Neurosci 30:16137–16148.

Swanson GT, Kamboj SK, Cull-Candy SG (1997) Single-channel properties of recombinant AMPA receptors depend on RNA editing, splice variation, and subunit composition. J Neurosci 17:58–69.

Tabatadze N, Huang G, May RM, Jain A, Woolley CS (2015) Sex differences in molecular signaling at inhibitory synapses in the hippocampus. J Neurosci 35:11252–11265.

Tanaka J, Matsuzaki M, Tarusawa E, Momiyama A, Molnar E, Kasai H, Shigemoto R (2005) Number and density of AMPA receptors in single synapses in immature cerebellum. J Neurosci 25:799–807.

Teyler TJ, Vardaris RM, Lewis D, Rawitch AB (1980) Gonadal steroids: effects on excitability of hippocampal pyramidal cells. Science 209:1017–1018.

Traynelis SF, Silver RA, Cull-Candy SG (1993) Estimated conductance of glutamate receptor channels activated during EPSCs at the cerebellar mossy fiber-granule cell synapse. Neuron 11:279–289.

Tuscher JJ, Szinte JS, Starrett JR, Krentzel AA, Fortress AM, Remage-Healey L, Frick KM (2016) Inhibition of local estrogen synthesis in the hippocampus impairs hippocampal memory consolidation in ovariectomized female mice. Horm Behav 83:60–67.

Watson JF, Ho H, Greger IH (2017) Synaptic transmission and plasticity require AMPA receptor anchoring via its N-terminal domain. Elife 6:e23024.

Whitehead G, Jo J, Hogg EL, Piers T, Kim DH, Seaton G, Seok H, Bru-Mercier G, Son GH, Regan P, Hildebrandt L, Waite E, Kim BC, Kerrigan TL, Kim K, Whitcomb DJ, Collingridge GL, Lightman SL, Cho K (2013) Acute stress causes rapid synaptic insertion of Ca^{2+}-permeable AMPA receptors to facilitate long-term potentiation in the hippocampus. Brain 136:3753–3765.

Wong M, Moss RL (1992) Long-term and short-term electrophysiological effects of estrogen on the synaptic properties of hippocampal CA1 neurons. J Neurosci 12:3217–3225.